JREE: Vol. 10, No. 1, (Winter 2023) 68-82

Journal of Renewable Energy and Environment

Journal Homepage: www.jree.ir

Materials and Energy Research Center

MERC

Research Article

Investigation of a Set of Novel Heat Exchanger Configurations of a Heat Recovery Steam Generator to Improve the Energy Efficiency of Combined Cycle Power Plant

Mohammad Rasooli Mavini [a], Hassan Ali Ozgoli [b*], Sadegh Safari [a]

[a] *Department of Energy Engineering, Faculty of Natural Resources and Environment, Science and Research Branch, Islamic Azad University (IAU), P. O. Box: 14515-775, Tehran, Tehran, Iran.*

[b] *Department of Mechanical Engineering, Iranian Research Organization for Science and Technology (IROST), P. O. Box: 33535-111, Tehran, Tehran, Iran.*

PAPER INFO

Paper history:
Received: 24 January 2022
Revised in revised form: 08 May 2022
Scientific Accepted: 28 May 2022
Published: 28 September 2022

Keywords:
HRSG,
CHP,
Configuration Analysis,
Energy Efficiency,
Environment Analysis

ABSTRACT

In this study, various configuration designs of a Heat Recovery Steam Generator (HRSG) are examined to enhance the energy efficiency of a Combined Cycle Power Plant (CCPP). A novel approach to investigating ten applicable configurations of a dual pressure HRSG is used thoroughly to explore the best practice models from the energy-conserving perspective. Further, a fuel consumption assessment has been conducted to identify the best performance of the cycle and investigate the minimum pollutants released by each Heat Recovery Steam Generator (HRSG). The results revealed that four out of ten scenarios expressed considerably better performance in terms of fuel consumption, steam production, energy efficiency, and environmental considerations. Further, it was found that compared to conventional configurations, not only the selected scenarios managed to improve the low-pressure steam generation, but also 30 % fuel consumption saving in supplementary firing was achieved as both economic and environmental benefits. Moreover, the carbon dioxide saving potential for the best scenario is 51.37 $kgCO_2$ MWh^{-1}; consequently, the environmental benefit of it is calculated to be about 133,418 $ MWh^{-1}.

https://doi.org/10.30501/jree.2022.326260.1317

1. INTRODUCTION

The upsurging consumption of fossil fuel has sparked some serious environmental problems on the global scale. Enhancing efficiency and mitigating pollutants are considered as the main concerns in any design of power generation plants. Therefore, improvement of thermal efficiency and reduction of fuel consumption of conventional cycles have gained much attention in tackle climate crises. There is no doubt that a Heat Recovery System (HRS), at any stage, plays a key role in conserving energy, not to mention the pivotal role of a Heat Recovery Steam Generator (HRSG) that is widely used as a critical component in various types of Combined Cycles (CC) [1]. Research on minimizing energy consumption and developing combined power generation systems in order to achieve better performance has deep roots in the literature [2, 3]. Some studies have highlighted the significance of recovering waste heat [4] and energy [5] into the cycle to improve energy efficiency, while many efforts have been made in the case of industrial sectors [6, 7]. Moreover, employing renewable energy sources in thermal cycles as well as using modern technologies such as gasifiers [8], fuel cells [9], and storage systems [10, 11] have attracted the attention of many researchers. In previous literature, it is widely considered as a good way to supply the required fuel of thermal and power systems using renewable resources such as biomass and biogas to mitigate the environmental consequences [12]. Ultimately, the application of integrated cycles such as Combined Heat and Power (CHP) and poly-generation systems has been considered as a significant purpose of optimizing energy consumption and reducing environmental issues associated with the Combined Cycle Power Plants (CCPPs) [13], given that these systems are still broadly adopted as a key player in supplying electricity demand in every corner of the world. The main reason behind this broad application is ample resources of the Nature Gas (NG) which is available in huge amount and it gives higher overall thermal efficiency [14]. Given that the Heat Recovery Steam Generatior (HRSG) is an indispensable part of these cycles and its function is to recover the waste heat present in the exhaust gases of the gas turbine and to generate the steam to run a steam power cycle, it is broadly highlighted in previous studies. Table 1 lists a review of the literature regarding the optimum performance analysis of CCPPs. It offers the design parameters, objectives, examination method, and the outstanding results and observations.

different positions from the conventional arrangement. Moreover, effective parameters in the best feasible layout will

*Corresponding Author's Email: a.ozgoli@irost.org (H.A. Ozgoli)
URL: https://www.jree.ir/article_158101.html

Please cite this article as: Rasooli Mavini, M., Ozgoli, H.A. and Safari, S., "Investigation of a set of novel heat exchanger configurations of a heat recovery steam generator to improve the energy efficiency of combined cycle power plant", ***Journal of Renewable Energy and Environment (JREE)***, Vol. 10, No. 1, (2023), 68-82. (https://doi.org/10.30501/jree.2022.326260.1317).

be selected by considering the environmental aspects as the main algorithm. Various heat exchanger layouts of the HRSG in a CCPP have been investigated to examine the maximum amount of generated steam at different pressure levels. In this regard, assessing the fuel consumption to identify the best performance of the cycle and investigating the minimum pollutants released of each HRSG configuration are accomplished.

Table 1. Literature review of optimum performance analysis of CCPPs

Design parameters	Considerations	Examination approach	Key Findings	Ref.
Mass flow rate, HRSG inlet gas temperature	Cycle efficiency	Thermodynamic and parametric analyses	Increasing the inlet gas to the HRSG until 650 °C is favorable. Increase in this temperature reduces the efficiency.	[15]
Temperature, steam pressure and pinch point	Energetic and exegetic efficiency	Thermodynamic methodology	By increasing the pinch point, the power to heat ratio also increases; however, the first-law and second-law efficiency decreases while the pinch point increases. Also, reheat process has received considerable improvement in output power and thermal power production.	[16]
pressure ratio, cycle temperature ratio, number of reheats and cycle pressure drop	Power-output, thermal efficiency, and exergy destruction	Thermodynamic analysis using second law	The efficiency and power output reach maximum at an intermediate pressure ratio. 50 % of the overall cycle exergy destruction occurs in the combustion chamber.	[17]
Operating conditions and cost related to fuel consumption, investment, and maintenance	Cost, and mass flowrate	Thermo-economic optimization using genetic algorithm	Various methods are investigated to establish how to reduce the objective function.	[18]
Mass flow rate, HRSG inlet gas temperature and pressure	Increasing efficiency over than 60 % without resorting new GT	Thermodynamic analysis and parametric study	Optimization of HRSG is sufficient to obtain the efficiency of a CCPPs in the order of 60 %. Gas to gas recuperation enhances the overall efficiency to 65 %.	[19]
Turbine Inlet Temperature (TIT), and pinch points the steam turbine inlet pressure	Optimization of the triple-pressure reheat combined cycle, irreversibility reduction of a HRSG	Thermodynamic analysis and parametric study	Optimal triple-pressure reheat CC is 1.7 % higher in efficiency than the reduced irreversibility triple-pressure reheat CC.	[20]
Inlet temperature to HRSG, pressure level, cost	HRSG pressure levels on exergy efficiency of combined cycle power plants	Thermo-economic optimization	Exergy destruction rate in HRSG is affected by an increase in the number of pressure levels and causes sensible improvement in exergy efficiency of the whole cycle.	[21]
Compression ratio, stack temperature and cooling steam ratio, temperature values of turbine inlet	Overall thermal efficiency and power output of the GT cycle were optimized	Thermodynamics optimization	The combined cycle gas turbine plants indicates better power output at 400 MW.	[22]
Ambient conditions	Electricity power generation and consumption of the fuel of the gas turbine cycle	Thermodynamic and parametric analysis	In comparison to the annual production in ISO conditions, the loss in electricity generation is about 2.87-0.71 %.	[23]
Steam quality at steam turbine outlet	Overall output power and efficiency	Multi-Objective Optimization (MOO) for the comprehensive thermodynamic analysis	The steam turbine inlet temperature and pressure increase when the steam quality at the steam turbine outlet increases.	[24]

A challenging problem that arises in this domain is the optimization of HRSG which not only is significantly important for the design of CCPPs but also plays a particular role in maximizing the power delivered to the Steam Turbine (ST) and improves the overall performance of the power cycle. As discussed earlier, achieving higher electric and thermal efficiency of the CCPPs requires optimizing the entire plant, and the three key components comprising the Gas Turbine (GT), HRSG, and Steam Turbine (ST). However, among the three mentioned component plants, the performance of the GT is of priority as the predominant influencer in the performance; most of the previous research studies in this field aim to solve this problem. However, the HRSG has rarely been studied directly. Furthermore, few studies have focused on different configurations of it as the HRSG component of the CCPPs can be made on order particularly for each GT unit, while the GT and ST can be selected from the set of commercially available range plants [24].

Based on the aforementioned explanations, no comprehensive study has been performed on the optimal configuration of heat exchangers in the HRSG system, so far. In the proposed new approach, the arrangement of HRSG heat exchangers in terms of thermal efficiency has been evaluated simultaneously with the electrical efficiency of the whole CCPP. The mathematical model described in this study makes it possible to determine the optimal configuration of the HRSG heat exchanger. In this way, heat exchangers of each pressure level can be placed in.

2. MATERIAL AND METHOD

2.1. System description

Figure 1 shows a chemotic flow diagram of a dual-pressure CCGT Power Plant. A CCGT Power Plant, generally, can be divided into three major subsystems: upstream cycle (Brayton cycle), downstream cycle (Rankin cycle), and HRSG. The system also includes other auxiliary equipment such as a pump, condenser, and cooling tower. In the upstream cycle, fresh air enters the compressor where compressed and leaves with higher temperature and pressure than the inlet point. In the combustion chamber, the compressed air and fuel, typically Natural Gas (NG) or diesel fuels, contribute to the combustion reaction. Then, combustion products will be expanded in the gas turbine for both generating electrical power employing generator and producing mechanical work for running the compressor. Further, the hot exhaust gas flow of GT, which is still capable of doing work, enters into the HRSG. In this study, there are several heat exchangers in dual pressure HRSG to use the thermal energy of this stream by passing through steps in the economizer, evaporator, and super heater. Eventually, superheat steam is produced to run High-Pressure (HP) and Low-Pressure (LP) steam turbines. The steam turbine sends its energy to the generator drive shaft, where it is converted into additional electricity.

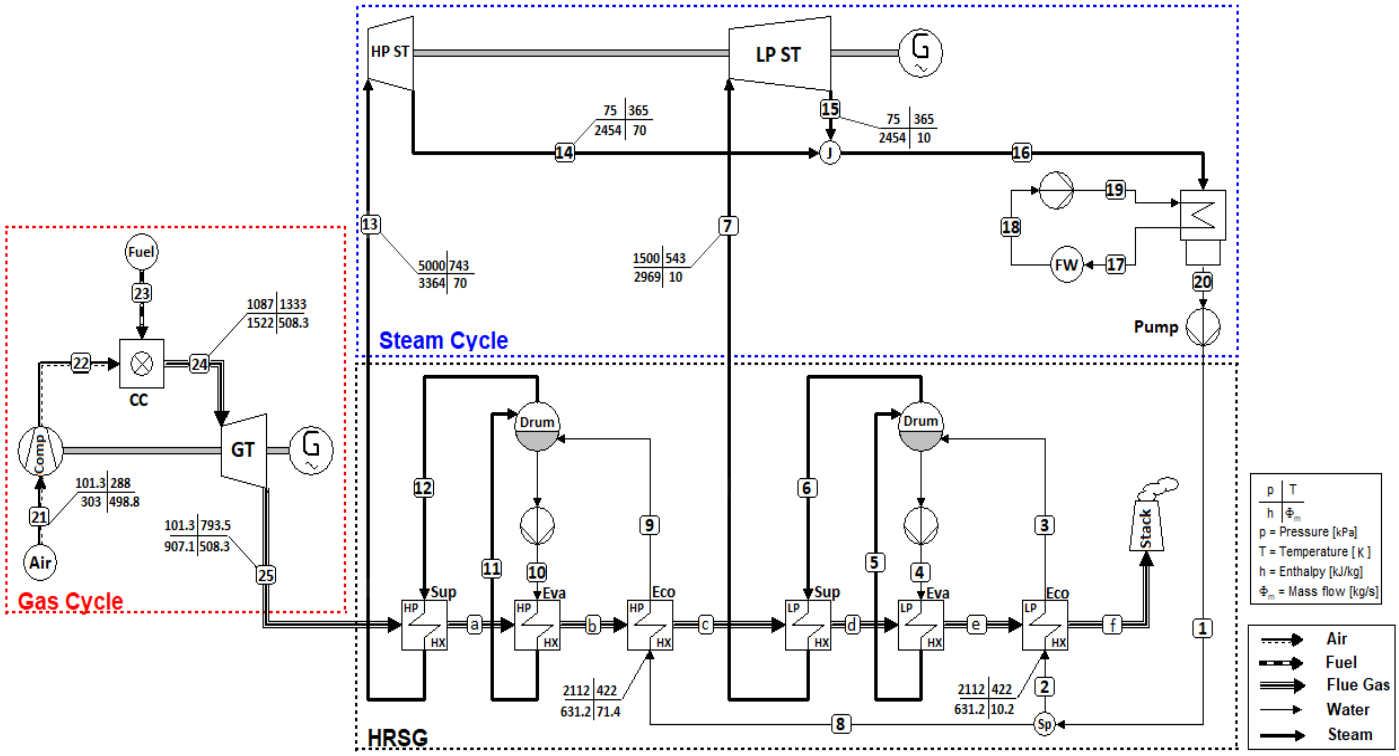

Figure 1. Schematic flow diagram of a dual-pressure CCGT power plant

2.2. Model assumptions

Several principal assumptions are considered to solve the model of the CCGT Power Plant. These assumptions which simplify the developed model and accelerate the calculation process are listed as follows:

- All processes have been done in a steady flow and steady-state conditions.
- Natural gas is considered as supplied fuel to the system.
- The ISO ambient condition (Temperature of 288 K and pressure of 101.3 kPa) is assumed.
- Siemens GT-V94.2 is used in Bryton Cycle.
- 5 % pressure drop is presumed in the both combustion chamber and HRSG.
- The HRSG unit is considered as a two-pressured unit.
- The blowdown of HP and LP drums is assumed 2 %.
- AP is considered to be characterized by 15 degrees.
- 0.86 and 0.90 are assumed as isentropic efficiency of compressor and isentropic efficiency of gas turbine, respectively.

These assumptions are employed throughout the analysis to derive the corresponding equations of each system component [18, 25, 26].

2.3. System modeling

The model was developed in Engineering Equation Solver (EES), which provided thermodynamic properties required to model and evaluate the performance of the CCGT Power Plant. For simplification, the calculation process model is divided into three major subsystems. Then, these sections are connected to provide an appropriate basis for both thermodynamic and environmental analyses of the system.

Further, first, the system subsections including compression and combustion, Gas Turbinr, dual-pressure HRSG, and Steam Turbine are explained by considering such design parameters as Compressor Pressure Ratio (CPR), Turbine Inlet Temperature (TIT), electricity power demand, blowing down amounts of high- and low-pressure drums, HP, and LP steam temperature and superheat approach temperature difference. Next, the environmental model is discussed. This study developed a mathematical model of an industrial gas turbine, validated the results through comparison of the actual performance of the Fars CCGT power plant located in Iran, and employed the same Siemens V94.2 turbines to produce electricity. Of note, the mentioned GT model is vastly used in the majority of power plants in Iran.

2.3.1. Combined cycle gas turbine power plant

In order to perform energetic analysis on the CCGT Power Plants, it is required to consider equations that are dominant at each component of the cycle. The equations regarding Compressor, Gas Turbine (GT), and Combustion Chamber (CC) are briefly presented in Table 2 [25].

Table 1. Governing equations on CCGT power plant [25]

CCGT power plant relations	Equations No.
$T_{AC_{out}} = T_{AC_{in}}\left\{1 + \frac{1}{\eta_{AC}}\left[RPC^{\frac{\gamma_{air}-1}{\gamma_{air}}} - 1\right]\right\}$	(1)
$\dot{w}_{AC} = \dot{m}_{air} C_{p_{air}}\left(T_{AC_{out}} - T_{AC_{in}}\right)$	(2)
$C_p = a + b\frac{T}{100} + c\left(\frac{T}{100}\right)^{-2}$	(3)
$a = \sum_{i=1}^{noc} a_i \times mf_i$	(4)
$b = \sum_{i=1}^{noc} b_i \times mf_i$	(5)
$c = \sum_{i=1}^{noc} c_i \times mf_i$	(6)
$RPC = \frac{P_{out}}{P_{in}}$	(7)
$\text{Heat Rate} = \frac{3412}{\eta_{th}} \quad \left[\frac{Btu}{kWh}\right]$	(8)
$\dot{m}_{Fuel} = \frac{PW_{GT} \times \text{Heat Rate}}{LHV}$	(9)
$O_{2_{theo}} = [2CH_4 + 3.5C_2H_6 + 5C_3H_8 + 6.5C_4H_{10} + 8C_5H_{12}] \times \dot{m}_{Fuel}$	(10)
$\dot{m}_{air_{theo}} = \frac{O_{2_{theo}}}{0.21} \times MW_{air}$	(11)
$\dot{m}_{air_{Act}} = \dot{m}_{air_{theo}} \times \left(\frac{\text{Excess Air \%}}{100} + 1\right)$	(12)
$T_{GT_{out}} = T_{GT_{in}}\left\{1 - \eta_{GT}\left[1 - RPT^{\frac{1-\gamma_{FG}}{\gamma_{FG}}}\right]\right\}$	(13)
$\dot{w}_{GT} = \dot{m}_g C_{p_{FG}}\left(T_{GT_{in}} - T_{GT_{out}}\right)$	(14)
$RPT = RPC \times (1 - \Delta P)$	(15)
$\dot{Q} - \dot{W} = \sum \dot{m}_{out} h_{out} - \sum \dot{m}_{in} h_{in}$	(16)
$H_{AC_{in}} = a\left(T_{AC_{in}} - T_{Ref}\right) + \frac{b}{100}\left({T_{AC_{in}}}^2 - \left(T_{AC_{in}} \times T_{Ref}\right)\right) + c(100)^2\left(\frac{1}{T_{AC_{in}}} - \frac{T_{Ref}}{{T_{AC_{in}}}^2}\right) + H_{Ref}$	(17)
$S_{AC_{in}} = a\ln\left(\frac{T_{AC_{in}}}{T_{Ref}}\right) + \frac{b}{100} \times T_{AC_{in}} \times \ln\left(\frac{T_{AC_{in}}}{T_{Ref}}\right) + c(100)^2\left(\frac{1}{{T_{AC_{in}}}^2}\right)\ln\left(\frac{T_{AC_{in}}}{T_{Ref}}\right) - R_{air}\ln\left(\frac{P_{AC_{in}}}{P_{Ref}}\right) + S_{Ref}$	(18)
$S'_{AC_{out}} = a\ln\left(\frac{T'_{AC_{out}}}{T_{AC_{in}}}\right) + \frac{b}{100} \times T'_{AC_{out}} \times \ln\left(\frac{T'_{AC_{out}}}{T_{AC_{in}}}\right) + c(100)^2\left(\frac{1}{{T'_{AC_{out}}}^2}\right)\ln\left(\frac{T'_{AC_{out}}}{T_{AC_{in}}}\right) - R_{air}\ln\left(\frac{P_{AC_{out}}}{P_{AC_{in}}}\right) + S_{AC_{in}}$	(19)
$\eta_{AC_{isen}} = \frac{H'_{AC_{out}} - H_{AC_{in}}}{H_{AC_{out}} - H_{AC_{in}}}$	(20)
$\dot{m}_{CC_{out}} h_{CC_{out}} = \dot{m}_{CC_{in}} h_{CC_{in}} + \dot{m}_{Fuel} \times \left[(\eta_{CC} \times LHV) + \left(C_{p_{Fuel}} \times T_{Fuel}\right)\right]$	(21)
$H_{GT_{in}} = a'\left(T_{GT_{in}} - T_{AC_{out}}\right) + \frac{b'}{100}\left({T_{GT_{in}}}^2 - \left(T_{GT_{in}} \times T_{AC_{out}}\right)\right) + c'(100)^2\left(\frac{1}{T_{GT_{in}}} - \frac{T_{AC_{out}}}{{T_{GT_{in}}}^2}\right) + H_{AC_{out}}$	(22)

$S_{GT_{in}} = a' \ln\left(\frac{T_{GT_{in}}}{T_{AC_{out}}}\right) + \frac{b'}{100} \times T_{GT_{in}} \times \ln\left(\frac{T_{GT_{in}}}{T_{AC_{out}}}\right) + c'(100)^2 \left(\frac{1}{T_{GT_{in}}^{\ 2}}\right) \ln\left(\frac{T_{GT_{in}}}{T_{AC_{out}}}\right) - R_{FG} \ln\left(\frac{P_{GT_{in}}}{P_{AC_{out}}}\right) + S_{AC_{out}}$	(23)
$S'_{GT_{out}} = a' \ln\left(\frac{T'_{GT_{out}}}{T_{GT_{in}}}\right) + \frac{b'}{100} \times T'_{GT_{out}} \times \ln\left(\frac{T'_{GT_{out}}}{T_{GT_{in}}}\right) + c'(100)^2 \left(\frac{1}{T'^{\ 2}_{GT_{out}}}\right) \ln\left(\frac{T'_{GT_{out}}}{T_{GT_{in}}}\right) - R_{FG} \ln\left(\frac{P_{GT_{out}}}{P_{GT_{in}}}\right) + S_{GT_{in}}$	(24)
$H'_{GT_{out}} = a'\left(T'_{GT_{out}} - T_{GT_{in}}\right) + \frac{b'}{100}\left(T'^{\ 2}_{GT_{out}} - \left(T'_{GT_{out}} \times T_{GT_{in}}\right)\right) + c'(100)^2 \left(\frac{1}{T'_{GT_{out}}} - \frac{T_{GT_{in}}}{T'^{\ 2}_{GT_{out}}}\right) + H_{GT_{in}}$	(25)
$\eta_{GT_{isen}} = \frac{H_{GT_{in}} - H_{GT_{out}}}{H_{GT_{in}} - H'_{GT_{out}}}$	(26)

Here, the RPC term in Equation (7) is the ratio of outlet air pressure to inlet air pressure that, according to the specifications of Siemens GT-V94.2, is equal to 11.31 [26]. To calculate the consumed fuel in a combustion chamber with regard to the heat rate, Equations (8) and (9) are used as follows [26]; then, the combustion equations can be written and solved as demonstrated in Equations (10-12) [26]. After solving Equations (8-12), required oxygen for combustion reaction will be obtained. Finally, by considering excess oxygen which is used to ensure complete combustion and increase mass flow rate, the actual amount of oxygen and air suction in the compressor will be obtained [26]. Since our work is always extracted from the expanding high pressure gas in the gas turbine system, outlet temperature and generated work are determined using Equations (13) to (15) [26, 27]. Further, the mass and energy balance equations for each component can be obtained from Equations (16) [26]. The calculation of enthalpy of flow in the inlet and outlet of each component is required for each correspondent equation of mass and energy balance as well as other cycle's components [26]. The enthalpy and entropy of the hot stream entering the gas turbine are obtained from Equations (22-25) [26].

Based on Equation (26) and isentropic efficiency of the gas turbine, the actual enthalpy of exhausted flow from the gas turbine can be obtained. The actual temperature of the outlet flow in the gas turbine as well as the entropy of the outlet stream from the gas turbine are in operating condition. Then, by considering the enthalpy of flow at the inlet and outlet of the gas turbine, the produced work by the turbine can be calculated using Equation (14) and in relation to the cycle. Finally, the net power generated by Gas Cycle (GC) as well as thermal efficiency of the gas cycle can be obtained by means of Equations (27) and (28), respectively [26].

$$W_{net_{GC}} = W_{GT} - W_{AC} \tag{27}$$

$$\eta_{th_{GC}} = \frac{W_{net_{GC}}}{Q_{in}} \tag{28}$$

In the steam cycle, the generated work by turbines can be obtained based on energy equation. With having pre-defined temperature and pressure of steam in LP and HP superheated conditions, the enthalpy of steams can be calculated. Then, by employing Equation (29), the work of steam turbine can be obtained. Further, according to the description given above, the net efficiency of the combined cycle power plant is calculated from integration of gas turbine cycle and steam cycle as described in Equations (30) to (32) [19, 26].

$$W_{ST} = \dot{m}_{HP}(h_{HP_{in}} - h_{HP_{out}}) + \dot{m}_{LP}(h_{LP_{in}} - h_{LP_{out}}) \tag{29}$$

$$\eta_{ST} = \frac{w_{ST} - w_{Pump}}{Q_{in_{ST}}} \tag{30}$$

$$\eta_{CCPP} = \frac{w_{GT} - w_{AC} + w_{ST} - w_{Pump}}{Q_{in_{CCPP}}} \tag{31}$$

$$\eta_{Electrical} = \frac{w_{GT} - w_{AC} + w_{ST}}{Q_{in_{CCPP}}} \tag{32}$$

2.3.2. Dual pressure HRSG

Two paths for exchanging heat in HRSG should be considered. The first path is where the hot exhausted gas flow from the gas turbine enters the HRSG unit and it moves towards the stack and eventually vents into the environment after passing through the exchanger tubes inside it. The second path is where the entering water to the HRSG unit passes through the inside of heat exchanger tubes until it is turned to superheated steam which will drive the steam turbine. In the base scenario of (A), for modeling superheated part and high-pressure evaporator, the following equations are employed [25]:

$$\begin{aligned} \dot{m}_{FG} \times C_{p_{FG}} \times (T_a - T_c) &= \dot{m}_{HP}(h_{12} - h_{11}) + \dot{m}_{HP}(h_{11} - h_9) \\ &+ \dot{m}_{HP}(1 + BLD_{HP}\,\%)(h_9 - h_8) \end{aligned} \tag{33}$$

In addition, for high-pressure economizer, low-pressure super heater, and the evaporator, we have Equation (34) as follows [25]:

$$\begin{aligned} \dot{m}_{FG} \times C_{p_{FG}} \times (T_c - T_f) &= \dot{m}_{HP}(1 + BLD_{HP}\,\%)(h_8 - h_7) \\ &+ \dot{m}_{LP}(h_6 - h_5) + \dot{m}_{LP}(h_5 - h_3) \\ &+ \dot{m}_{LP}(1 + \%\,BLD_{LP})(h_3 - h_2) \end{aligned} \tag{34}$$

Through Equations (33) and (34), the production values of high-pressure and low-pressure superheated steam will be obtained [24].

$$\begin{aligned} \dot{m}_{DB} \times C_{p_{FG}} \times (T_{c_{new}} - T_f) &= \dot{m}'_{HP}(1 + BLD_{HP}\,\%)(h_8 - h_7) \\ &+ \dot{m}'_{LP}(h_6 - h_5) + \dot{m}'_{LP}(h_5 - h_3) \\ &+ \dot{m}'_{LP}(1 + BLD_{LP}\,\%)(h_3 - h_2) \end{aligned} \tag{35}$$

After calculating the corrected temperature at point C, the HRSG input temperature is modified through Equation (36) [25]:

$$\dot{m}_{DB} \times C_{p_{FG}} \times \left(T_{a_{new}} - T_{c_{new}}\right) = \dot{m}'_{HP}(h_{12} - h_{11}) + \dot{m}'_{HP}(h_{11} - h_9) + \dot{m}'_{HP}(1 + BLD_{HP}\,\%)(h_9 - h_8) \quad (36)$$

In the end, the temperature of the inlet flow into the HRSG that should produce the amount of required steam at different pressure levels will be determined. Also, by solving the mass and energy balance equations for the duct burner, the amount of auxiliary fuel that provides the supplementary firing system will be calculated. Then, the amount of air for delivering complete combustion can be calculated.

$$\dot{m}_{FG} \times h_{GT_{out}} + \dot{m}_{FA} \times h_{FA} + \dot{m}_{Ax_{Fuel}} \times \left(LHV + \left(C_{p_{Fuel}} \times T_{Fuel}\right)\right) = \dot{m}_{DB} \times C_{p_{FG}} \times T_{a_{new}} \quad (37)$$

$$\dot{m}_{FA} = \frac{\dot{m}_{Ax_{Fuel}}}{MW_{Fuel}} \times 10.96 \times MW_{air} \quad (38)$$

$$\dot{m}_{DB} = \dot{m}_{FG} + \dot{m}_{FA} + \dot{m}_{Ax_{Fuel}} \quad (39)$$

2.4. Environmental modeling

The less a system generates CO_2 emissions, the more environmentally-friendly the plant is [12]. In order to analyze the combustion products, the combustion equation must first be written and solved for each compartment of fuel to obtain the quantities of combustion products. In this equation, the amount of carbon dioxide and argon in the combustion air has been monitored. According to the general combustion equation for fuel, the following equation is given [28].

$$C_xH_y + n \times \left(1 + \left(\frac{\text{Excess air }\%}{100}\right)\right) \times (O_2 + 3.72 \times N_2 + 0.04 \times AR + 0.0014 \times CO_2) = n_1 \times CO_2 + n_2 \times H_2O + n_3 \times N_2 + n_4 \times AR + n_5 \times O_2 \quad (40)$$

To evaluate the environmental expenses associated with CO_2 emissions in conventional systems, Equation (41) is simply employed [27]. Herein, $\dot{z}_{CO_2}$ is the environmental damage cost , $\dot{m}_{CO_2}$ potential emission of CO_2, and C_{CO_2} is the unit damage cost which is equal to 0.024 $/kg [29]. Therefore, the carbon emission saving potential of the present study can be calculated for each configuration design through Equation (42), where $\Omega_{CO_2 ref}$ is the CO_2 emission from a base scenario which is scenario (A) in this study. The environmental benefit (BEN_{env}) of the best scenario designed can be calculated using Equation (43) [8, 27].

$$\dot{z}_{CO_2} = \dot{m}_{CO_2} \times C_{CO_2} \quad (41)$$

$$\Omega_{CO_2 potential} = \Omega_{CO_2 ref} - \Omega_{CO_2 sys} \quad (42)$$

$$BEN_{env} = \dot{z}_{CO_2} \times \Omega_{CO_2 potential} \quad (43)$$

3. METHODOLOGY

3.1. Solution methodology

In this work, a solution methodology is illustrated and indicated in Figure 2. The key intention of the proposed methodology is to offer the operation solutions based on technical model for engineers. The technical proposed model will be solved in three consecutive steps by employing all the required equations in a structured manner, as illustrated in Figure 2. Later, power and efficiency of each component as well as the pollutant emission for the winner scenario as dependent variables will be determin.

3.2. Input parameters and validation

The model developed in the preceding sections is used to simulate and evaluate the performance of the CCGT power plant. The model input parameters of the Bryton cycle of the studied plant are listed in Table 3. More details may be found in [18, 26]. Initial values for the CCGT power plant are presented in Table 4 and more details can be found in [25, 26].

In order to ensure the model validation and accuracy, some modeling results of the CCGT power plant are compared to those of the installed CCGT power plant in south of Iran, and the results are shown in Table 5. It is observed that the presented results reasonably agree with the actual outcomes of the installed plants.

Besides, in Table 6, the values of the specific heat capacity have been calculated with minor difference from the measured values. As a result, the enthalpy of the flow can be accurately estimated. Thus, another major parameter of HRSG modeling, which is the enthalpy of hot gas flow entering it, was obtained with high accuracy.

3.3. Scenario description

Regarding the layout of heat exchangers in HRSG, 10 designed scenarios are presented and discussed in Table 7 labelled from (A) to (J). It is worth noting that among them, two scenarios of (G) and (H) have been presented and evaluated from different aspects in previous studies, whereas others are examined in the present study to explore the best configuration in terms of energy improvement. First of all, in scenario (A), a low-pressure economizer, evaporator, and super heater as well as a high-pressure economizer, evaporator, and super heater are arranged along the length of HRSG and from the end to the first part close to the outlet of the gas turbine, while in scenario (B), it is shown that they are in the same order, except that the high-pressure economizer is fed from the output of low-pressure economizer, as depicted schematically below. Next, in scenario (D), the same layout of scenario (C) is considered; however, as is shown earlier, the high-pressure economizer inlet will be supplied from the low-pressure economizer as previously discussed. For a better understanding of the scenarios, Figure 3 presents the base scenario and Table 7 shows the all scenarios and their associated changes.

Further, in scenario (E), low-pressure super heater is deliverd to the beginning part of HRSG ahead of HP superheater, while in scenario (F), the economizers are connected. Furthermore, in scenario (G), the high-pressure economizer is moved ahead of the low-pressure superheater and after the low-pressure evaporator. In scenario (H), the outlet of the low-pressure economizer is connected to the inlet of the high-pressure economizer with the same arrangement; in scenario (I), the low-pressure super heater is moved forward, but the other heat exchangers have the same arrangement of first scenario (A). Finally, in scenario (J), the inlet and outlet of economizers are connected.

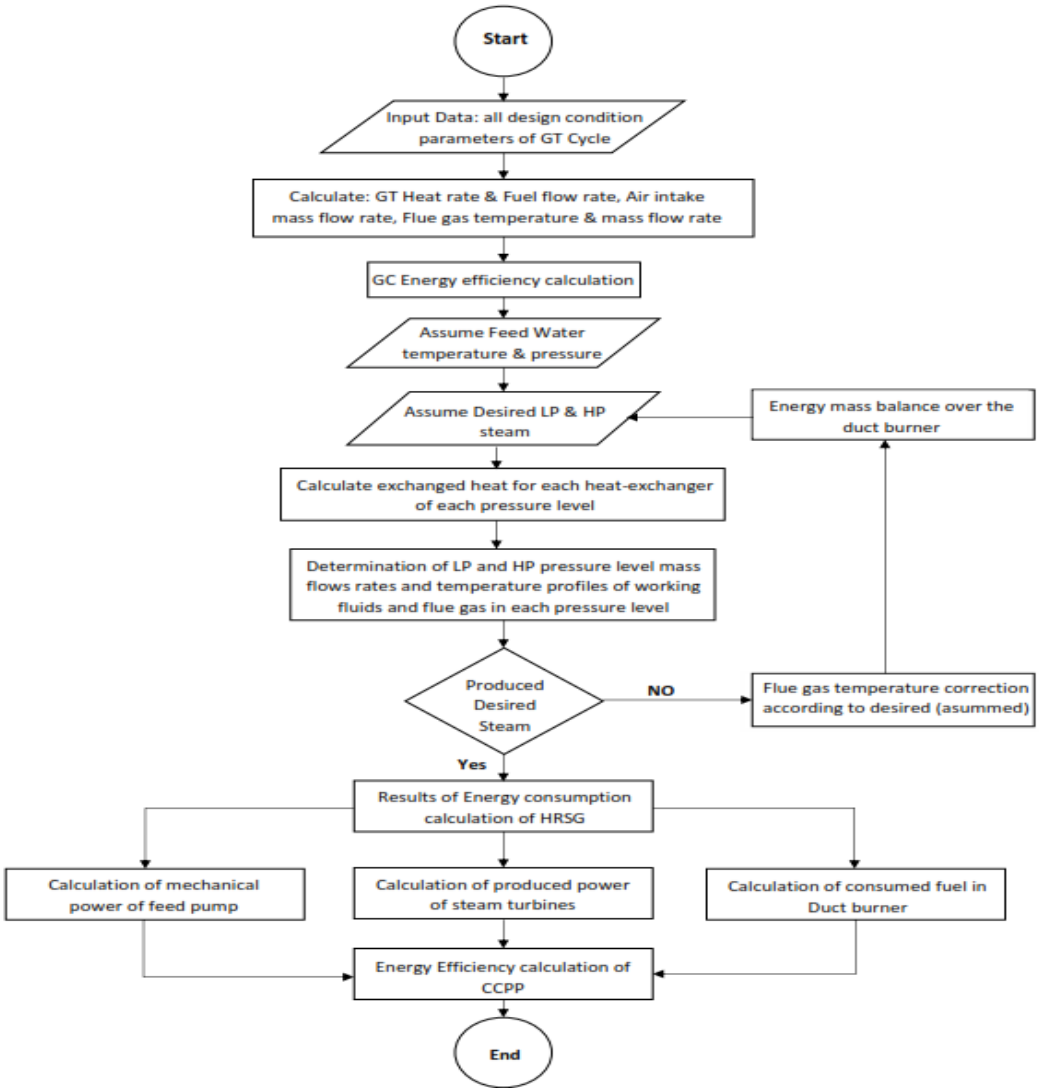

Figure 2. Solution procedure of the CCGT power plant model

Table 3. Model input parameters for the Brayton cycle [18, 26]

Parameters	Value	Unit
Compressor isentropic efficiency	87	%
Compressor flow rate	500	[kg/s]
Combustion chamber efficiency	99	%
Excess air	210	%
Fuel flow rate	9.56	[kg/s]
Pressure ratio of cycle	11.30	-
Pressure loss	5	%
Turbine isentropic efficiency	90	%
Turbine inlet temperature	1333	[K]

Table 4. Initial values for modeling of the presented CCPP

Parameter	Value	Unit
Electricity power demand	159,000	[kW]
Ambient air temperature	288.15	[K]
Ambient air pressure	101.30	[kPa]
Reference temperature	273.15	[K]
Reference pressure	101.30	[kPa]
Approach temperature	15	[K]
Fuel temperature	293.15	[K]

Table 5. Thermo-physical property of medium fluid in the BC

Items	Model results		Fars power plant		Relative error(%)
	Inlet	Outlet	Inlet	Outle	Outlet
Compressor					
Temperature [K]	304.95	626.9	304.9	629.95	0.48
Pressure [**kPa**]	101.30	1145	-	-	-
Mass flow rate [kg/s]	498.81	498.8	504.4	504.40	1.11
Enthalpy [kJ/kg]	303.01	647.5	305.3	640.51	-1.08
Combustion chamber					
Temperature [K]	594.3	1333	640	1333	0
Pressure [**kPa**]	1145	1087	-	-	-
Mass flow rate [kg/s]	498.8	508.3	504	513.5	1.01
Enthalpy [kJ/kg]	612.00	1522	-	-	-
Gas Turbine					
Temperature [K]	1333	796.7	1333	809.95	1.63
Pressure [**kPa**]	1087	101.3	-	-	-
Mass flow rate [kg/s]	508.3	508.3	513.5	513.50	1.01
Enthalpy [kJ/kg]	1522	907.1	-	873.24	-3.87

Table 6. The specific heat capacity comparison with Fars power plant

Specific heat	Calculated [J/kg. K]	Measured [J/kg. K]	Relative error (%)
N_2	1.037	1.039	0.19
O_2	0.910	0.916	0.65
Ar	0.521	0.520	-0.19
CO_2	0.827	0.835	0.95
Dry air	1.001	1.005	0.39

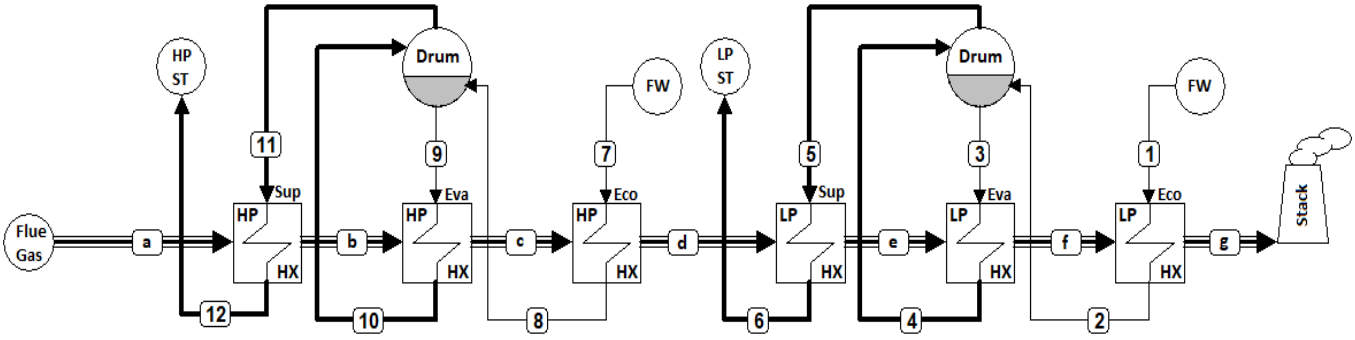

Figure 3. Base scenario of (A)

Table 7. Scenario comparison and highlighting the changes in each scenario with the previous one

Scenario comparison	Previous layout	New layout
Scn. B Vs. Scn. A	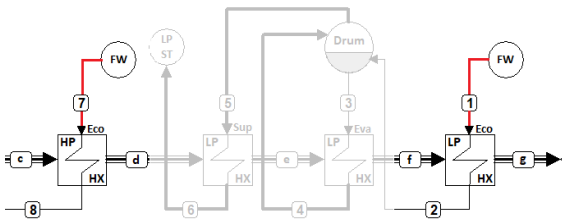	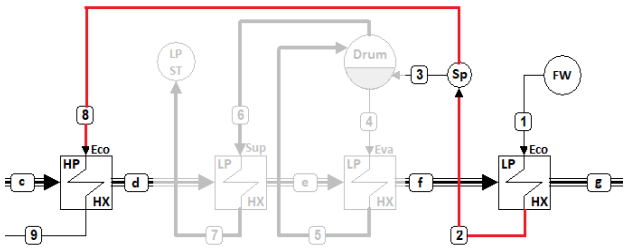
	Using low-pressure economizer preheated water for high-pressure economizer input	
Scn. C Vs. Scn. A	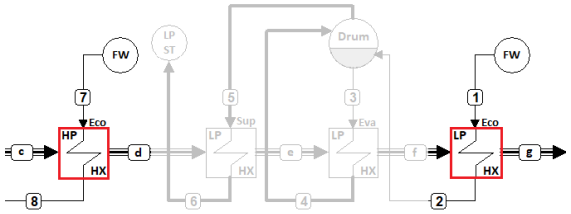	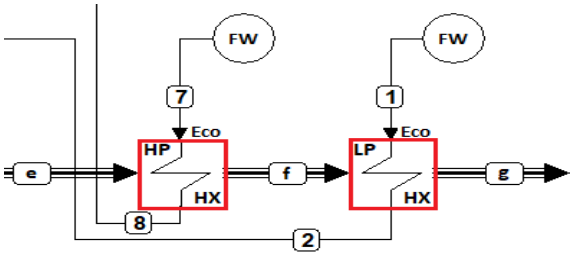
	Placement of high-pressure economizer after the low-pressure economizer	
Scn. D Vs. Scn. C	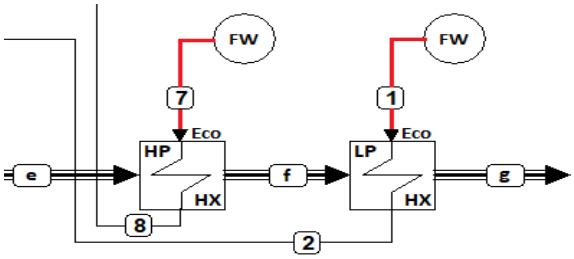	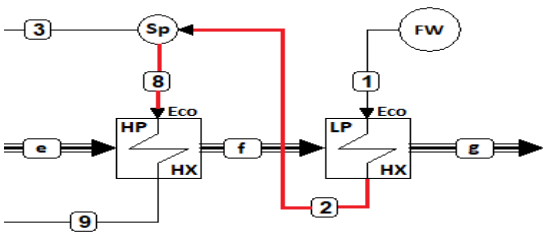
	Application of low-pressure economizer preheated water for high-pressure economizer input	

Scn.E Vs. Scn.A	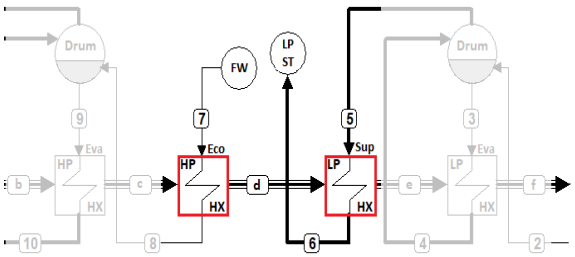	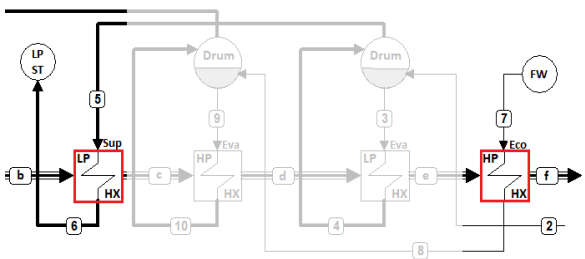
High-pressure economizer placement before low-pressure evaporator and low-pressure superheater after high-pressure evaporator		
Scn. F Vs. Scn. E	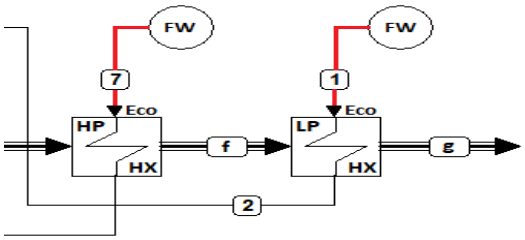	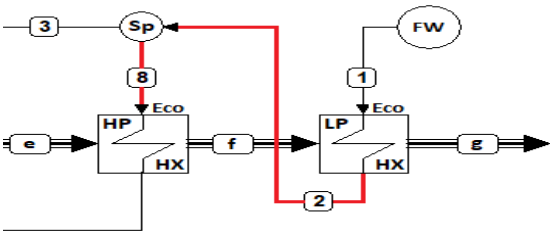
Using low-pressure economizer preheated water for high-pressure economizer input		
Scn. G Vs. Scn. A	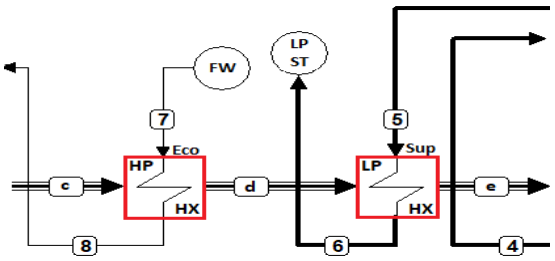	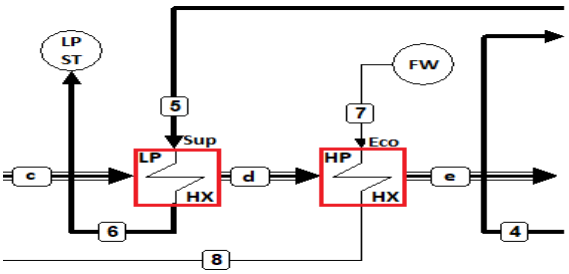
Placement of high-pressure economizer before the superheater		
Scn. H Vs. Scn G	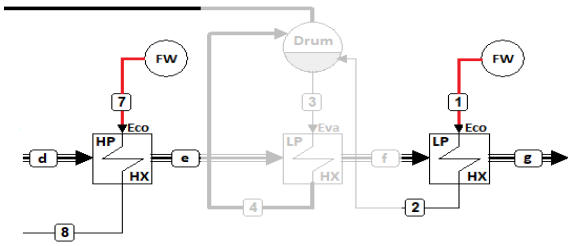	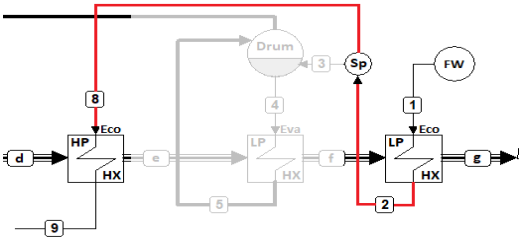
Using low-pressure economizer preheated water for high-pressure economizer input		
Scn. I Vs. Scn A	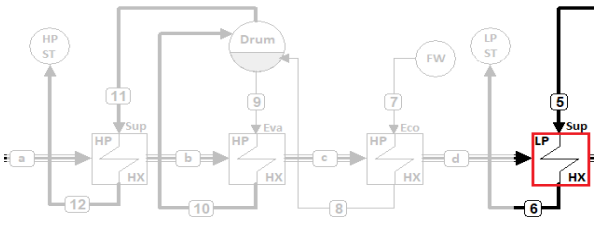	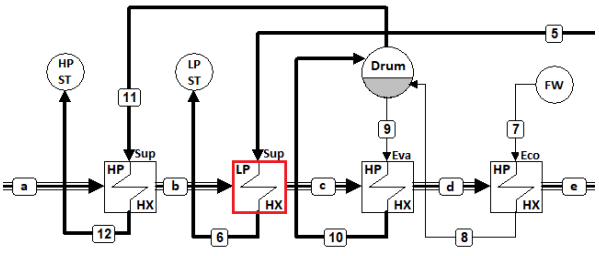
Low-pressure superheater placement before high-pressure superheater		
Scn. J Vs. Scn. I	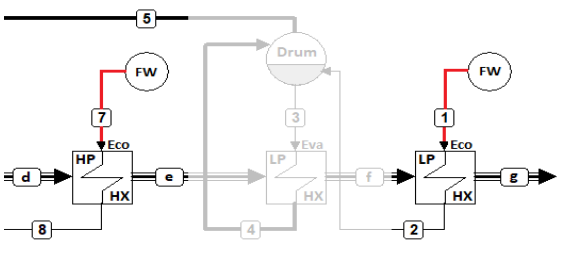	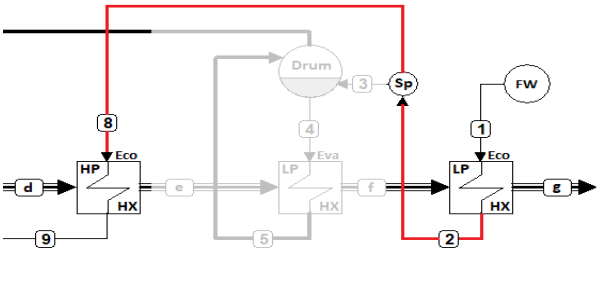
Using low-pressure economizer preheated water for the high-pressure economizer input		

4. RESULTS AND DISCUSSION

In this section, the effect of different heat exchanger arrangements based on various scenarios on the system performance is determined and thoroughly discussed. The temperatures of hot exhausted gas flow passing through the HRSG for all scenarios are presented in Table 8. Also, the thermodynamic properties of flue gas for the base scenario (A) are presented in Table 9 (A) and water and steam flows are presented in Table 9 (B).

Table 8. Flue gas temperature in each section of the proposed HRSG scenarios

Flue gas stream line	Scn. A T [K]	Scn. B T [K]	Scn. C T [K]	Scn. D T [K]	Scn. E T [K]	Scn. F T [K]	Scn. G T [K]	Scn. H T [K]	Scn. I T [K]	Scn. J T [K]
a	796.7	796.7	796.7	796.7	796.7	796.7	796.7	796.7	796.7	796.7
b	735.7	735.7	735.7	735.7	737.1	737.1	735.7	735.7	736.1	736.4
c	552.1	552.1	552.1	552.1	731.4	731.4	552.1	552.1	734.6	733.5
d	503.1	519.2	546.8	546.8	552.1	552.1	550.8	549.5	552.1	552.1
e	501.7	516.5	486.5	486.5	486.5	486.5	501.7	516.5	503.4	519.6
f	486.5	486.5	437.4	453.5	438.6	454.3	486.5	486.5	486.5	486.5
g	485.3	468.2	432.9	433.0	433.7	433.8	485.3	468.2	485.2	468.2

Table 9 (A). Gas thermodynamic properties of dual-pressure HRSG scenario (A)

Heat exchanger	T_{gi} [K]	T_{go} [K]	$M_{g,i}$ [kg/s]	Q [kJ]
LP Economizer	485.3	486.5	508.3	683
LP Evaporator	486.5	501.7	508.3	9116
LP Super heater	501.7	503.1	508.3	810
HP Economizer	503.1	552.1	508.3	29541
HP Evaporator	552.1	735.7	508.3	109077
HP Super heater	735.7	796.7	508.3	36743

Table 9 (B). Water & steam thermodynamic properties of dual-pressure HRSG

HP Stream	Temperature [°C]	Pressure [kPa]	Enthalpy [kJ/kg]	Mass flow rate [kg/s]
12	470.0	5000	3364	64.48
11	264.0	5000	2794	64.48
10	264.0	5000	2794	64.48
9	264.0	5000	1154	64.48
8	249.0	2112	1080	65.77
7	149.5	2112	631.2	65.77
LP Stream	**Temperature [°C]**	**Pressure [kPa]**	**Enthalpy [kJ/kg]**	**Mass flow rate [kg/s]**
6	270.0	1500	2969	4.56
5	198.3	1500	2792	4.56
4	198.3	1500	2792	4.56
3	198.3	1500	844.9	4.56
2	183.3	2112	778.0	4.65
1	149.5	2112	631.2	4.65

4.1. Steam generation evaluations at high pressure and low pressure in HRSG

A comparison of steam generation at high and low pressures in HRSG in each designed scenario is illustrated in Figure 4. As it can be clearly observed from the results, the scenarios (E) and (F) generate considerably more steam in the default state which is equal to approximately 20 kg/s at LP steam generation rate, while in worse scenarios which are (G) and (H), the LP steam generation rates correspond to 4.56 kg/s. The main reason behind this is the suitable arrangement of heat exchangers within the HRSG. It is worth noting that the steam produced in scenarios (E) and (F) is substantially greater than that in scenario (A) which is a presented conventional layout of heat exchangers in the HRSG. Moreover, LP steam production of scenarios (G) and (H) which are studied and suggested in the previous literature is considerably lower than that in the proposed scenarios in this study. Superior results conspicuously result from the proposed scenarios of (E) and (F) as they demonstrate the highest levels of LP steam production.

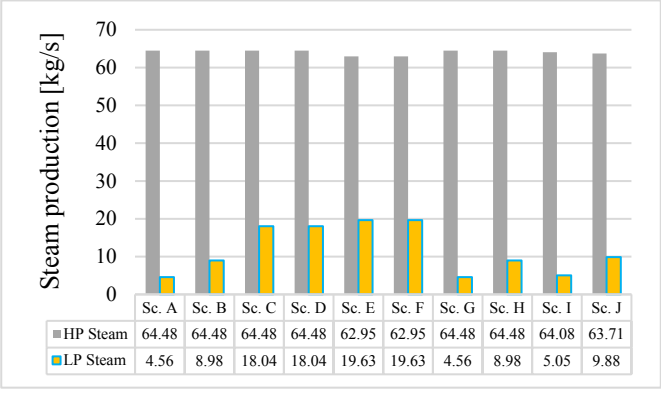

Figure 4. LP & HP steam generation in different scenarios without duct burner

4.2. Fuel consumption of duct burner for steam generation

There is no doubt that fuel consumption in the thermal systems is of particular interest of examination to not only achieve higher efficiency but also lessen the operation cost as well as environmental side effects associated with it. Considering that all HRSG scenarios are designed to produce

a specific amount of steam at specific pressures as illustrated in Table 1, the supplemental firing unit enables the system to track demand (i.e., producing more steam when the load swings upward than the unfired unit can produce). The duct burner must compensate for providing needed heat (temperature and mass flow rate) to the stream passing through the HRSG. If the heat rate at HRSG is not sufficient to generate a specific amount of steam, it operates to provide the required energy using auxiliary fuel.

In Table 10, fuel consumption of different configurations of HRSG with and without supplemental firing unit is illustrated. As can be observed, maximum fuel consumption belongs to scenarios (A), (G), and (I) in which duct burner used 1.055 kg/s while superior results regarding fuel consumption belonged to scenarios (C), (D), (E), and (F) where duct burner consumed 0.317 kg/s and total amount of fuel consumption was equal to 9.884 kg/s to produce a specific and stable amount of steam at HP and LP pressures. This delivers significantly better results due to low fuel consumption corresponding to about 7 % saving in fuel. The main reason behind this fuel saving can be more efficient heat exchanger arrangement in related scenarios. This achievement can be more tangible when it comes to annual scale which immensely improves operation costs and mitigates the environmental side effects, finally resulting in huge annual cost saving.

Table 10. Fuel consumption of CCGTs power plant in different configurations of dual-pressure HRSG

Scenarios	Fuel consumption (kg/s)	Gas turbine (kg/s)	Duct curner (kg/s)
A	10.622	9.567	1.055
B	10.38	9.567	0.813
C	9.884	9.567	0.317
D	9.884	9.567	0.317
E	9.884	9.567	0.317
F	9.884	9.567	0.317
G	10.622	9.567	1.055
H	10.38	9.567	0.813
I	10.622	9.567	1.055
J	10.38	9.567	0.813

Also, scenarios (B), (C), and (I) exhibit better results than the base scenario (A). The total fuel consumption in the mentioned scenarios is 10.38 kg/s, which corresponds to approximately 3 % saving.

4.3. Electrical power and efficiency

The power generation capacity of the steam cycle in both high-pressure and low-pressure steam turbines regarding different scenarios is illustrated in Figure 5. As can be seen, scenarios (C) and (D) produced maximum power in the steam cycle equal to 68.54 MW that causes approximately 12 % improvement in comparison with scenario (A) where it generates 61.17 MW. This enhancement is mainly due to better performance in low-pressure steam turbine power production which increased from 2.5 MW to 9.87 MW.

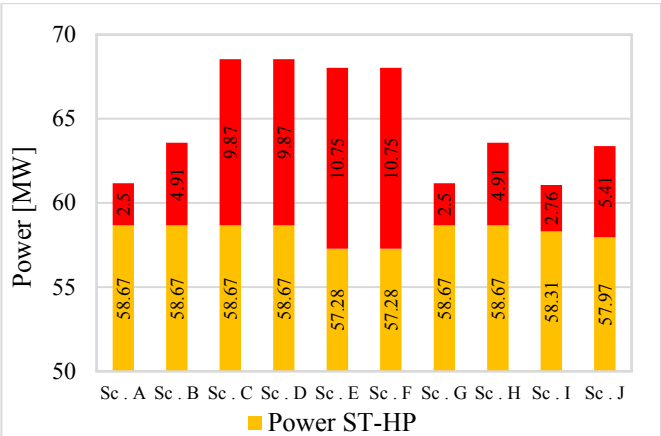

Figure 5. Power production of steam cycle considering different scenarios

Further, scenarios (A), (G), and (I) exhibited approximately similar performance, while slight improvements can be seen in scenarios (B) and (H). An improvement in total steam production from 61.17 MW to 63.58 MW can be observed. This delivers significantly better results due to a more efficient heat exchanger arrangement in the HRSG.

Figure 6 shows the total net power production in both GC and SC for different proposed scenarios. As discussed earlier, from obtained results, it can be clearly understood that scenarios (C) and (D) had a greater level of power production equal to 218.33 MW. Also, it should be noted that the scenario (I), the most unfavorable one, can produce the net electrical power of 210.89 MW.

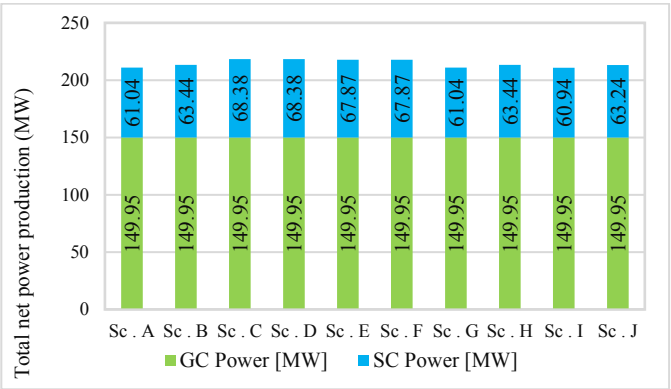

Figure 6. Total net power production of gas gycle and steam cycle for different scenarios

Total net power and efficiency of CCPP, GC, and ST for different designed scenarios are illustrated in Figure 7. As can be seen, the designed heat exchanger arrangement of scenario

(C) has not only the best thermal and electrical efficiency of the system, but also produces the maximum power of 218.3 MW, while the scenario (A) produces 210.98 MW electricity. Based on a comparison of different scenarios, it was found that the best performance in both power and efficiency belonged to scenarios (C) and (D).

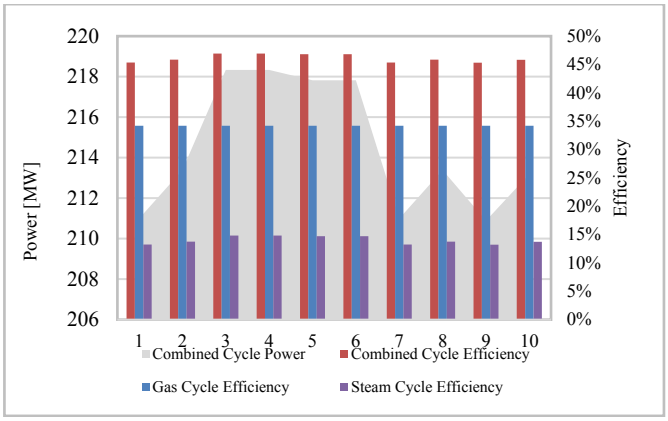

Figure 7. Total net power and efficiency of CCPP, GC, and ST for different scenarios

Further, Figure 8 shows a comparison between produced and consumed power in two scenarios (A) as base configuration and scenario (C) as the best designed heat exchanger arrangement. As is illustrated in two pie charts, the most striking difference in power production is related to the low-pressure steam turbine power production in scenario (C), which is remarkably enhanced due to new configuration design.

The low-pressure steam turbine power generation is improved from 2.5 MW in base scenario (A) to 9.87 MW in the best scenario (C) where the power production in low-pressure steam cycle has been approximately quadrupled. In addition, overall power production of CCPP has been significantly improved from 210.98 MW to 218.3 MW, while consumed fuel has proved to be almost 7 % saving potential. The energy consumption in compressor is maintained constant, as expected.

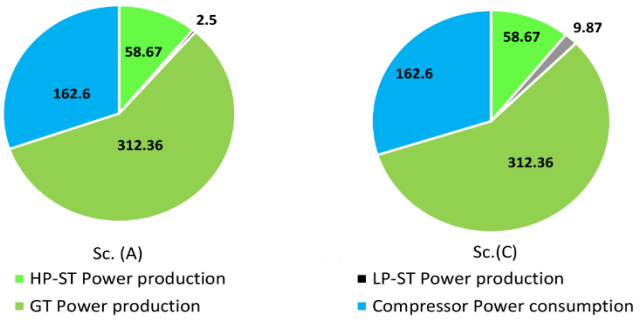

Figure 8. A comparison between produced and consumed power in scenarios (A) and (C)

In addition, the two T-Q diagrams with regard to scenarios of (A) as base configuration and scenario (C) as the best performed scenario are shown in Figures 9 and 10, respectively.

According to Figure 9, the GT hot flue gas at point (a) is incorporated into the HRSG at a temperature of 796.7 K and after passing LP as well as HP units leave the HRSG unit at point (g) with a temperature of 485.4 K. At the same time, feed water enters the HRSG unit at points (g) and (d). Moreover, after heat exchange, the superheat steam will leave the unit at the point (d) with a temperature of 543.2 K for LP-steam and at the point of (a) with a temperature of 743.2 K for HP-steam.

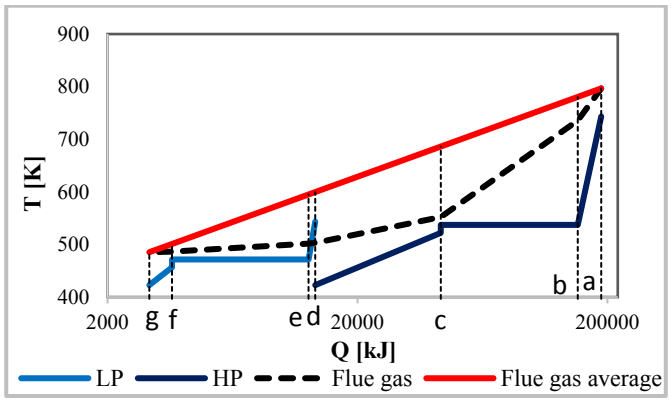

Figure 9. T-Q profile of scenario (A)

This diagram clearly shows the amount of heat exchanged in each heat exchanger. It is observed that the highest amount of heat exchange belongs to the HP section of the HRSG and the highest value is in the HP evaporator heat exchanger. By comparing the temperature profile of hot flue gas passing through the HRSG from point (a) to (g) and temperature profiles of produced steam, it can be observed that there is still a great energy potential to be recovered and saved from the outlet gases. The higher the energy recovery is, the closer the temperature profile of the steam produced is to the temperature profile of the hot gas.

Figure 10 shows the temperature profile of scenario (C). It can be seen that in this scenario, compared to the base scenario (A), the steam temperature profile is much closer to the outlet gas temperature profile, which means higher and more efficient heat exchange and, consequently, more heat recovery from the hot outlet-gas flow. In scenario (C), the outlet gas temperature declines to 432.9 K, where its temperature is reduced by almost 53 K in comparison to the base scenario. Besides, in the LP unit, more heat is observed rather than the base scenario which leads to more steam production at 295.6 %. Ultimately, more power will be produced in the LP-steam turbine of the CCGT power plant.

By comparing these two diagrams, it is concluded that by changing the configuration of heat exchangers in HRSG, the amount of heat exchanged between the hot stream (flue gas from the gas turbine) and the cold streams (high-pressure and low-pressure steam flows) increases. This value will be at the highest possible value due to the minimization of the pinch point temperature difference.

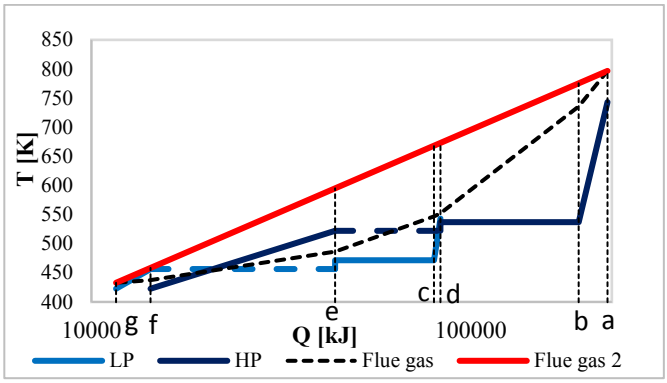

Figure 10. T-Q profile of scenario (C)

5. ENVIROMENTAL ASSESSMENT

It is necessary to assess the environmental effects on thermal and power generation systems that generally provide their required energy using fossil fuels. In this study, the amount of fuel combustion products at the combined cycle power plant for a scenario with the lowest fuel consumption is studied and the results are presented in Table 11.

In terms of environmental analysis, the benefits of the proposed configurations are investigated and compared with the environmental damage triggered by a base scenario of (A) as reference. The CO_2 emission cost rate of the scenario (C) is about 461.521 $\mathrm{kgCO_2/MWh}$ which is considerably lower than the base scenario which is equal to 512.89 $\mathrm{kgCO_2/MWh}$. Moreover, $\Omega_{\mathrm{CO_2 potential}}$ of the system is 51.37 $\mathrm{kgCO_2/MWh}$; consequently, $\mathrm{BEN_{Env}}$of the system is equal to 133,418 $/MWh. Accordingly, for fuel consumption of 10.61 kg/s in base configuration of gas turbine cycle with HRSG, scenario (A), the amount of 30.06 $\mathrm{kgCO_2/s}$ is generated, equal to 2597 ton/day. Since the designed configurations in scenarios (C), (D), (E), and (F) have the lowest fuel consumption, lower CO_2 production of about 2418 ton is the result. This value shows 178.8 ton/day reduction in comparison with the base scenario of (A).

Table 11. Calculated flue gas components of gas turbine for all the proposed scenarios

Component	Value Sc. A [kg/s]	Value Sc. B [kg/s]	Value Sc. C [kg/s]	Value Sc. D [kg/s]	Value Sc. E [kg/s]	Value Sc. F [kg/s]	Value Sc. G [kg/s]	Value Sc. H [kg/s]	Value Sc. I [kg/s]	Value Sc. J [kg/s]
CO_2	30.06	29.38	27.99	27.99	27.99	27.99	30.06	29.38	30.06	29.38
H_2O	22.31	21.80	20.76	20.76	20.76	20.76	22.31	21.80	22.31	21.80
O_2	78.38	78.38	78.38	78.38	78.38	78.38	78.38	78.38	78.38	78.38
N_2	390.4	387.3	381.0	381.0	381.0	381.0	390.4	387.3	390.4	387.3
Ar	5.986	5.939	5.843	5.843	5.843	5.843	5.968	5.939	5.986	5.939

5. CONCLUSIONS

Scenario base modeling was undertaken for different dual-pressure HRSG configurations considering operational flue gas temperature and related initial values that represent the new evaluation approach of combined cycles. The expressed scenarios were selected due to the steam demand of the considered power plant and the technical possibility of the heat exchanger arrangement. Therefore, the primary purpose of this study was to present a method to increase the productivity of the HRSG systems. Results demonstrated that four of the ten considered HRSG models had a better operation in fuel consumption, steam production, power, and electrical efficiency than the conventional configuration. Besides, the environmental benefit of the best scenario proved to be a remarkable improvement. Eventually, concerning the HRSG model development, low-pressure steam generation of the scenarios of (C), (D), (E), and (F) was about four times higher than that in the base scenario of (A). It was shown that more energy could be absorbed in the HRSG by relocating super heaters and evaporators of the LP section. So, the following outputs were obtained:

- Fuel consumption of duct burner of the selected configurations was almost 30 % less than the conventional type.
- HRSG efficiency using four selected configurations was approximately 9 % higher than the base model.
- Reduction of CO_2 emission in the best scenario of (C) was about 6.88 % in comparison with the base model.
- The environmental benefit of the best scenario was equal to 133,418 $/MWh.

6. ACKNOWLEDGEMENT

The authors appreciatively acknowledge the Iranian Research Organization for Science and Technology (IROST) for providing the input data of Fars power plant.

NOMENCLATURE

Symbols	
a, b, c	Specific heat constants of steam
a', b', c'	Specific heat constants of flue gas
BLD	Blow down (%)
C_p	Specific heat capacity at constant pressure (kJ/kg K)
dT	Temperature division
h	Specific enthalpy (kJ/kg)
H	Enthalpy at actual state (kJ)
H'	Enthalpy at ideal state (kJ)
LHV	Lower heating value (kJ/kg)
mf	Mass fraction
$\dot{m}$	Mass flow rate (kg/s)
$\dot{m}'$	Demand mass flow rate (kg/s)
$\dot{m}$ole	Mole flow rate (kmole/s)
MW	Molecular weight (kg/kmole)
n	Mole of air in combustion reaction (kmole)
$n_1, \ldots, n_5$	Mole of products in combustion reaction (kmole)
P	Pressure (bar)
PW	Power (kW)
Q	Heat transferred (kJ)
$\dot{Q}$	Heat transferred rate (kJ/kg)
R	Gas constant (kJ/kg K)
RPC	Compressor pressure ratio
RPT	Turbine pressure ratio
S	Entropy at actual state (kJ/kg K)
S'	Entropy at ideal state (kJ/kg K)
T	Temperature at actual state (K)
T'	Temperature at ideal state (K)
W	output work (kJ)
$\dot{W}$	Specific output work (kJ/kg)
ΔP	Pressure difference (%)
Greek Letter	
η	Efficiency
γ	Specific heat ratio
Subscripts and superscripts	
air	Air
AC	Air compressor
Act	Actual
CC	Combustion chamber

CCPP	Combined cycle power plant
DB	Duct burner
Demand	Demand
Electrical	Electrical
Fuel	Fuel
FA	Fresh air
FG	Flue gas
FW	Feed water
GC	Gas cycle
GT	Gas Turbine
HP	High pressure
Eco	Economizer
Sup	Super heater
Sp	Splitter
HX	Heat Exchanger
in	Inlet
isen	Isentropic state
LP	Low pressure
net	Net
new	New state
out	Outlet
p	Pump
Ref	Reference
ST	Steam turbine
th	Thermal
theo	Theoretical
0	Initial state

Acronyms and abbreviation

AP	Approach point temperature
CCPP	Combined cycle power plant
CHP	Combined heat and power
EES	Engineering equation solver
LP	Feed water
PP	Gas turbine
HP	High pressure
HRSG	Heat recovery steam generator
LP	Low pressure
PP	Pinch point
TIT	Turbine inlet temperature
TOT	Turbine outlet temperature

REFERENCES

1. Moghadasi, M., Ozgoli, H.A. and Farhani, F., "A machine learning-based operational control framework for reducing energy consumption of an amine-based gas sweetening process", ***International Journal of Energy Research***, Vol. 45, No. 1, (2021), 1055-1068. (https://doi.org/10.1002/er.6159).
2. Ozgoli, H.A. and Ghadamian, H., "Energy price analysis of a biomass gasification-solid oxide fuel cell-gas turbine power plant", ***Iranian Journal of Hydrogen & Fuel Cell***, Vol. 3, No. 1, (2016), 45-58. (https://doi.org/10.22104/ijhfc.2016.327).
3. Ozgoli, H.A., Safari, S. and Sharifi, M.H., "Integration of a biomass-fueled proton exchange membrane fuel cell system and a vanadium redox battery as a power generation and storage system", ***Sustainable Energy Technologies and Assessments***, Vol. 42, (2020), 100896. (https://doi.org/10.1016/j.seta.2020.100896).
4. Moghadasi, M., Ozgoli, H.A. and Farhani, F., "Gas sweetening process simulation - Investigation on recovering waste hydraulic energy", ***International Journal of Mechanical, Industrial and Aerospace Sciences***, Vol. 12, No. 8, (2018), 789-804. (https://doi.org/10.5281/zenodo.1340566).
5. Ozgoli, H.A., Elyasi, S. and Mollazadeh, M., "Hydrodynamic and electrochemical modeling of vanadium redox flow battery", ***Mechanics & Industry***, Vol. 16, No. 2, (2015), 201-213. (https://doi.org/10.1051/meca/2014071).
6. Ozgoli, H.A., Ghadamian, H. and Farzaneh, H., "Energy efficiency improvement analysis considering environmental aspects in regard to biomass gasification PSOFC/GT power generation system", ***Procedia Environmental Sciences***, Vol. 17, (2013), 831-841. (https://doi.org/10.1016/j.proenv.2013.02.101).
7. Ozgoli H.A., Moghadasi, M., Farhani, F. and Sadigh, M., "Modeling and simulation of an integrated gasification SOFC-CHAT cycle to improve power and efficiency", ***Environmental Progress & Sustainable Energy***, Vol. 36, No. 2, (2016), 610-618. (https://doi.org/10.1002/ep.12487).
8. Safari, S., Ghasedi, A.H. and Ozgoli, H.A., "Integration of solar dryer with a hybrid system of gasifier-solid oxide fuel cell/micro gas turbine: Energy, economy, and environmental analysis", ***Environmental Progress & Sustainable Energy***, Vol. 40, No. 3, (2020), e13569. (https://doi.org/10.1002/ep.13569).
9. Safari, S., Hajilounezhad, T. and Ehyaei, M.A., "Multi-objective optimization of solid oxide fuel cell/gas turbine combined heat and power system: A comparison between particle swarm and genetic algorithms", ***International Journal of Energy Research***, Vol. 44, No. 11, (2020), 9001-9020. (https://doi.org/10.1002/er.5610).
10. Ozgoli, H.A. and Yazdani, H., "Integration of a vanadium redox flow battery with a proton exchange membrane fuel cell as an energy storage system", ***Iranian Journal of Hydrogen and Fuel Cell***, Vol. 1, (2017), 53-68. (https://doi.org/10.22104/ijhfc.2017.2281.1140).
11. Abanades, S., Abbaspour, H., Ahmadi, A., Das, B., Ali Ehyaei, M., Esmaeilion, F., El Haj Assad, M., Hajilounezhad, T., Hmida, A., Rosen, M.A., Safari, S., Shabi, M.A. and Silveira, J.L., "A conceptual review of sustainable electrical power generation from biogas", ***Energy Science & Engineering***, Vol. 10, No. 2, (2021), 630-655. (https://doi.org/10.1002/ese3.1030).
12. Ozgoli, H.A., "Simulation of integrated biomass gasification-gas turbine-air bottoming cycle as an energy efficient system", ***International Journal of Renewable Energy Research***, Vol. 7, No. 1, (2017), 276-284. (https://doi.org/10.20508/ijrer.v7i1.5428.g6986).
13. Ozgoli, H.A., Ghadamian, H. and Pazouki, M., "Economic analysis of biomass gasification-solid oxide fuel cell-gas turbine hybrid cycle", ***International Journal of Renewable Energy Research***, Vol. 7, No. 3, (2017), 1007-1018. (https://doi.org/10.20508/ijrer.v7i3.5814.g7131).
14. Safari, S. and Ozgoli, H.A., "Electrochemical modeling and techno-economic analysis of solid oxide fuel cell for residential applications", ***Journal of Renewable Energy and Environment (JREE)***, Vol. 7, No. 1, (2020), 40-50. (https://doi.org/10.30501/jree.2020.105451).
15. Kaviri, A.G., Jaafar, M.N.M., Lazim, T.M. and Barzegaravval, H., "Exergoenvironmental optimization of heat recovery steam generators in combined cycle power plant through energy and exergy analysis", ***Energy Conversion and Management***, Vol. 67, (2013), 27-33. (https://doi.org/10.1016/j.enconman.2012.10.017).
16. Kumar, A., Kachhwaha, S. and Mishra, R., "Thermodynamic analysis of a regenerative gas turbine cogeneration plant", ***Journal of Scientific and Industrial Research***, Vol. 69, No. 3, (2010), 225-231. (http://nopr.niscpr.res.in/bitstream/123456789/7384/1/JSIR%2069%283%29%20225-231.pdf).
17. Khaliq, A. and Kaushik, S.C., "Second-law based thermodynamic analysis of Brayton/Rankine combined power cycle with reheat", ***Applied Energy***, Vol. 78, No. 2, (2004), 179-197. (https://doi.org/10.1016/j.apenergy.2003.08.002).
18. Ahmadi, P. and Dincer, I., "Thermodynamic analysis and thermoeconomic optimization of a dual pressure combined cycle power plant with a supplementary firing unit", ***Energy Conversion and Management***, Vol. 52, No. 5, (2011), 2296-2308. (https://doi.org/10.1016/j.enconman.2010.12.023).
19. Franco, A. and Casarosa, C., "On some perspectives for increasing the efficiency of combined cycle power plants", ***Applied Thermal Engineering***, Vol. 22, No. 13, (2002), 1501-1518. (https://doi.org/10.1016/S1359-4311(02)00053-4).
20. Bassily, A.M., "Modeling, numerical optimization, and irreversibility reduction of a triple-pressure reheat combined cycle," ***Energy***, Vol. 32, No. 5, (2007), 778-794. (https://doi.org/10.1016/j.energy.2006.04.017).
21. Tajik Mansouri, M., Ahmadi, P., Ganjeh Kaviri, A. and Mohd Jaafar, M.N., "Exergetic and economic evaluation of the effect of HRSG configurations on the performance of combined cycle power plants", ***Energy Conversion and Management***, Vol. 58, (2012), 47-58. (https://doi.org/10.1016/j.enconman.2011.12.020).
22. Antonanzas, J., Alía Martínez, M., Ascacibar, F.J. and Antonanzas, F., "Towards the hybridization of gas-fired power plants: A case study of Algeria", ***Renewable and Sustainable Energy Reviews***, Vol. 51, (2015), 116-124. (https://doi.org/10.1016/j.rser.2015.06.019).
23. Erdem, H. and Sevilgen, S., "Case study: Effect of ambient temperature on the electricity production and fuel consumption of a simple cycle gas

turbine in Turkey", ***Applied Thermal Engineering***, Vol. 26, (2006), 320-326. (https://doi.org/10.1016/j.applthermaleng.2005.08.002).

24. Ibrahim, T.K., Kamil Mohammed, M., Awad, O.I., Rahman, M.M., Najafi, G., Basrawi, F., Abd Alla, A.N. and Mamat, R., "The optimum performance of the combined cycle power plant: A comprehensive review", ***Renewable and Sustainable Energy Reviews***, Vol. 79, (2017), 459-474. (https://doi.org/10.1016/j.rser.2017.05.060).
25. Feng, H., Zhong, W., Wu, Y. and Tong, S., "Thermodynamic performance analysis and algorithm model of multi-pressure heat recovery steam generators (HRSG) based on heat exchangers layout", ***Energy Conversion and Management***, Vol. 81, (2014), 282-289. (https://doi.org/10.1016/j.enconman.2014.02.060).
26. Razak, A.M.Y., Industrial gas turbines, 1st Edition, Woodhead Publishing, Elsevier, (2007), 624-650.
27. Ahmadi, A., Das, B., Ehyaei, M.A., Esmaeilion, F., El Haj Assad, M., Jamali, D.H., Koohshekan, O., Kumar, R., Rosen, M.A., Negi, S., Sekhar Bhogilla, S. and Safari, S., "Energy, exergy, and techno-economic performance analyses of solar dryers for agro products: A comprehensive review", ***Solar Energy***, Vol. 228, (2021), 349-373. (https://doi.org/10.1016/j.solener.2021.09.060).
28. Abanades, S., Abbaspour, H., Ahmadi, A., Das, B., Ehyaei, M.A., Esmaeilion, F., El Haj Assad, M., Hajilounezhad, T., Jamali, D.H., Hmida, A., Ozgoli, H.A., Safari, S., AlShabi, M. and Bani-Hani, E.H., "A critical review of biogas production and usage with legislations framework across the globe", ***International Journal of Environmental Science and Technology***, Vol. 19, (2022), 3377–3400. (https://doi.org/10.1007/s13762-021-03301-6).
29. Hosseinpour, J., Chitsaz, A., Liu, L. and Gao, Y., "Simulation of eco-friendly and affordable energy production via solid oxide fuel cell integrated with biomass gasification plant using various gasification agents", ***Renewable Energy***, Vol. 145, (2020), 757-771. (https://doi.org/10.1016/j.renene.2019.06.033).